

Search for the $\eta' \rightarrow e^+e^-$ decay with the SND detector

M.N. Achasov,^{1,2} V.M. Aulchenko,^{1,2} A.Yu. Barnyakov,^{1,2} K.I. Beloborodov,^{1,2}
 A.V. Berdyugin,^{1,2} D.E. Berkaev,^{1,2} A.G. Bogdanchikov,¹ A.A. Botov,¹ T.V. Dimova,^{1,2,*}
 V.P. Druzhinin,^{1,2} V.B. Golubev,^{1,2} L. V. Kardapoltsev,^{1,2} A.S. Kasaev,¹
 A.G. Kharlamov,^{1,2} A.N. Kirpotin,¹ D.P. Kovrizhin,^{1,2} I.A. Koop,^{1,2,3} A.A. Korol,^{1,2}
 S.V. Koshuba,^{1,2} A.S. Kupich,^{1,2} K.A. Martin,^{1,2} N.Yu. Muchnoi,^{1,2} A.E. Obrazovsky,¹
 A.V. Otboev,^{1,2} E.V. Pakhtusova,¹ A.I. Senchenko,^{1,2} S.I. Serednyakov,^{1,2}
 P.Yu. Shatunov,^{1,2} Yu.M. Shatunov,^{1,2} D.A. Shtol,¹ D.B. Shwartz,^{1,2} Z.K. Silagadze,^{1,2}
 I.K. Surin,¹ Yu.A. Tikhonov,^{1,2} Yu.V. Usov,^{1,2} A.V. Vasiljev,^{1,2} and I.M. Zemlyansky^{1,2}

(The SND Collaboration)

¹*Budker Institute of Nuclear Physics, SB RAS, Novosibirsk, 630090, Russia*

²*Novosibirsk State University, Novosibirsk 630090, Russia*

³*Novosibirsk State Technical University, Novosibirsk, 630092, Russia*

A search for the process $e^+e^- \rightarrow \eta'$ has been performed with the SND detector at the VEPP-2000 e^+e^- collider. The data were accumulated at the center-of-mass energy of 957.78 ± 0.06 MeV with an integrated luminosity of about 2.9 pb^{-1} . For reconstruction of the η' meson five decay chains have been used: $\eta' \rightarrow \eta\pi^+\pi^-$ followed by the η decays to $\gamma\gamma$ and $3\pi^0$, and $\eta' \rightarrow \eta\pi^0\pi^0$ followed by the η decays to $\pi^+\pi^-\pi^0$, $\gamma\gamma$, and $3\pi^0$. As a result, the upper limit has been set on the η' electronic width: $\Gamma_{\eta' \rightarrow e^+e^-} < 0.0020 \text{ eV}$ at the 90% confidence level.

PACS numbers: 13.20.Jf, 13.40.Gp, 13.66.Bc, 14.40.Be

I. INTRODUCTION

This article is devoted to a search for the rare leptonic decay $\eta' \rightarrow e^+e^-$. In the Standard model this decay proceeds through the two-photon intermediate state (Fig. 1) and, therefore, is suppressed as α^2 relative to the η' two-photon decay. An additional suppression

*baiert@inp.nsk.su

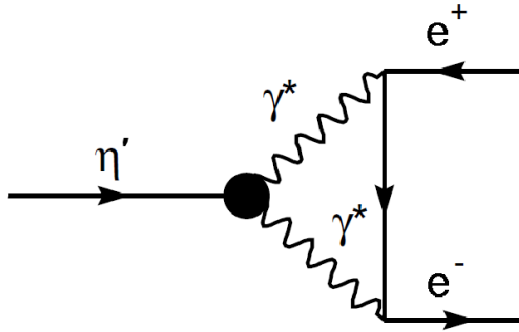


FIG. 1: The diagram for the $\eta' \rightarrow e^+e^-$ decay.

of $(m_e/m_{\eta'})^2$ arises from helicity conservation. The imaginary part of the $\eta' \rightarrow e^+e^-$ decay amplitude can be expressed in terms of the known two-photon width $\Gamma(\eta' \rightarrow \gamma\gamma)$. Neglecting the real part of the amplitude one can obtain the model-independent lower limit (unitary limit) on the decay probability $\mathcal{B}(\eta' \rightarrow e^+e^-) > 3.8 \times 10^{-11}$ [1]. Calculation of the real part requires knowledge of the transition form factor $F(q_1^2, q_2^2)$ for the $\gamma^*\gamma^* \rightarrow \eta'$ vertex, where q_1^2 and q_2^2 are the photon virtualities in the loop. The real part may increase the decay probability by a factor of 3–5 as compared with the unitary limit [2, 3]. Due to the small probability, the $\eta' \rightarrow e^+e^-$ decay may be sensitive to contributions not described by the Standard Model [4, 5].

The strictest limit on the decay branching fraction $\mathcal{B}(\eta' \rightarrow e^+e^-) < 1.2 \times 10^{-8}$ [6] at the 90% confidence level (CL) was set recently in the experiments with the CMD-3 detector at the VEPP-2000 e^+e^- collider [8]. In this experiment the technique of using the inverse reaction $e^+e^- \rightarrow \eta'$ for a measurement of $\mathcal{B}(\eta' \rightarrow e^+e^-)$ proposed in Ref. [7] was applied. The cross section of the $e^+e^- \rightarrow \eta'$ reaction at the center-of-mass (c.m.) energy $E = m_{\eta'}c^2$ is equal to

$$\sigma_0 = \frac{4\pi}{m_{\eta'}^2} B(\eta' \rightarrow e^+e^-). \quad (1)$$

In this paper we present the results of the search for the $\eta' \rightarrow e^+e^-$ decay in the experiments with the SND detector at the VEPP-2000 collider. The SND data used in this analysis were collected simultaneously with the CMD-3 data mentioned above.

II. DETECTOR AND EXPERIMENT

The SND detector is described in detail elsewhere [9]. This is a nonmagnetic detector, the main part of which is a three-layer spherical electromagnetic calorimeter based on NaI(Tl) crystals. The solid angle covered by the calorimeter is 90% of 4π . Its energy resolution for photons is $\sigma_E/E = 4.2\%/\sqrt[4]{E(\text{GeV})}$, and the angular resolution is about 1.5° . The directions of charged particles are measured by a tracking system, which consists of the 9-layer drift chamber and the proportional chamber with readout from cathode strips. The tracking system covers a solid angle of 94% of 4π . The calorimeter is surrounded by a muon system, which is used, in particular, for cosmic-background suppression.

Data used in this analysis with an integrated luminosity of about 2.9 pb^{-1} were accumulated in 2013 at the c.m. energy close to $m_{\eta'}c^2 = 957.78 \pm 0.06 \text{ MeV}$ [10]. During the data taking period the beam energy was monitored with an absolute accuracy of about 60 keV by the Back-scattering-laser-light system [11]. The data taking conditions are described in detail in Ref. [6]. The average value of the c.m. energy is $E_{\text{cm}} = 957.68 \pm 0.060 \text{ MeV}$; its spread is $\sigma_{E_{\text{cm}}} = 0.246 \pm 0.030 \text{ MeV}$. To obtain the cross section of η' production in the real experimental conditions we have to take into account the radiative corrections to the initial state, and the energy spread. This was done in Ref. [6]. As the collider energy spread (FWHM = 0.590 MeV) is significantly larger than the η' width $\Gamma_{\eta'} = (0.198 \pm 0.009) \text{ MeV}$ [10], the resulting cross section is proportional to the electronic width

$$\sigma_{\text{vis}}(\text{nb}) = (6.38 \pm 0.23)\Gamma_{\eta' \rightarrow e^+e^-}(\text{eV}). \quad (2)$$

It should be noted that the radiative corrections and the energy spread lead to a reduction of the cross section compared to the Born one (Eq. (1)) by a factor of four.

The search for the process $e^+e^- \rightarrow \eta'$ is performed in five decay chains: $\eta' \rightarrow \eta\pi^+\pi^-$ with the η decays to $\gamma\gamma$ and $3\pi^0$, and $\eta' \rightarrow \eta\pi^0\pi^0$ with the η decays to $\pi^+\pi^-\pi^0$, $\gamma\gamma$ and $3\pi^0$. For luminosity normalization of events with charged particles in the final state the large-angle Bhabha scattering is used, while for events containing only photons the luminosity is measured using the two-photon annihilation $e^+e^- \rightarrow \gamma\gamma$. The corresponding integrated luminosities are measured to be $L_{ee} = 2.91 \text{ pb}^{-1}$ and $L_{\gamma\gamma} = 2.82 \text{ pb}^{-1}$. The difference between these values, about 3%, gives us a conservative estimate of the luminosity systematic uncertainty.

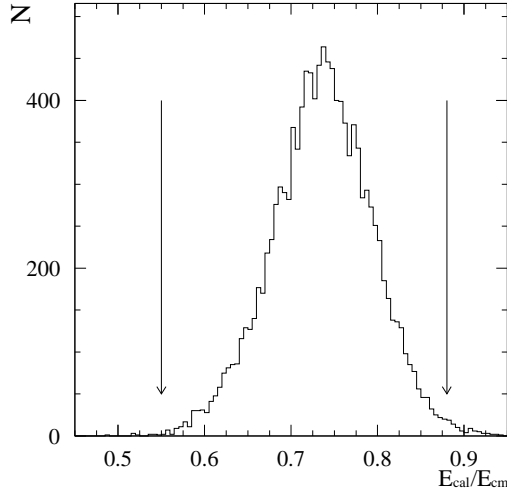


FIG. 2: The spectrum of the normalized total energy deposition in the calorimeter for simulated events of the process $e^+e^- \rightarrow \eta' \rightarrow \pi^+\pi^-\eta$, $\eta \rightarrow \gamma\gamma$. The arrows indicate the boundaries of the selection cut $0.55 < E_{\text{cal}}/E_{\text{cm}} < 0.9$.

Using different normalizations allows to partly cancel systematic uncertainties associated with hardware event selection, charged track reconstruction, and beam-generated extra tracks.

III. EVENT SELECTION

A. Decay chain $\eta' \rightarrow \pi^+\pi^-\eta$, $\eta \rightarrow \gamma\gamma$

This η' decay channel has the largest probability, about 17%, and the lowest multiplicity among the channels studied in this work. Because of the small multiplicity the background for this channel arises from almost all e^+e^- annihilation processes. In background processes with a small number of photons, as $e^+e^- \rightarrow e^+e^-(\gamma)$ or $e^+e^- \rightarrow \pi^+\pi^-(\gamma)$, additional fake photons appear as a result of splitting of electromagnetic showers, nuclear interaction of pions in the calorimeter, or superimposing beam-generated background.

At the first stage events with two charged particles originating from the interaction region and two photons are selected. The muon system veto is applied to reject cosmic-ray background. The charged particle tracks are fitted into a common vertex. Their polar angles must be in the range $40^\circ < \theta < 140^\circ$. To suppress background from collinear two-body processes, mainly from $e^+e^- \rightarrow e^+e^-$, the azimuthal angles of the charged particles are required

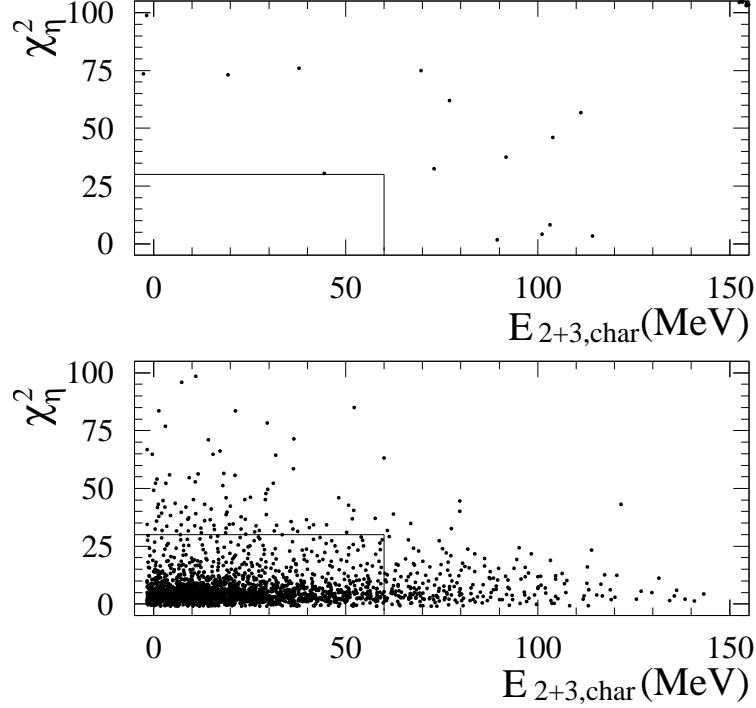


FIG. 3: Two-dimensional distribution of parameter χ_η^2 over $E_{\text{char},2+3}$ for data events (top) and simulated events of the $e^+e^- \rightarrow \eta' \rightarrow \pi^+\pi^-\eta$, $\eta \rightarrow \gamma\gamma$ process (bottom). The rectangle in the bottom left corner of the plot corresponds to the selection criteria $\chi_\eta^2 < 30$ and $E_{\text{char},2+3} < 60$ MeV.

to satisfy the condition $|180^\circ - |\phi_1 - \phi_2|| > 10^\circ$. The background from $e^+e^- \rightarrow n\gamma$ events with photon conversion into an e^+e^- -pair is rejected by the condition $\psi_{cc} > 20^\circ$, where ψ_{cc} is the open angle between the charged particles. To remove events with fake photons from pion nuclear interactions in the calorimeter, the condition on the minimal open angle between a charged particle and photon $\psi_{c\gamma} > 20^\circ$ is applied. The specific feature of this channel is a large energy deposition in the calorimeter E_{cal} . The distribution of this parameter for simulated events of the process $e^+e^- \rightarrow \eta' \rightarrow \pi^+\pi^-\eta \rightarrow \pi^+\pi^-2\gamma$ is shown in Fig. 2. The arrows indicate the boundaries of the condition used $0.55 < E_{\text{cal}}/E_{\text{cm}} < 0.9$.

For events passing preliminary selection the kinematic fit to the $e^+e^- \rightarrow \pi^+\pi^-\eta$ hypothesis is performed. The quality of the fit is characterized by the parameter χ_η^2 . Another important parameter used for the final selection is the sum of energy depositions of charged particles in the second and third layers of the calorimeter $E_{2+3,\text{char}}$. Since pions in the process under study are soft, they stop predominantly in the first layer of the calorimeter. The

two-dimensional distributions of the parameters χ_η^2 and $E_{2+3,\text{char}}$ for data events and simulated events of the process under study are shown at Fig. 3. The rectangle in the bottom left corner corresponds to the selection criteria applied: $\chi_\eta^2 < 30$ and $E_{\text{char},2+3} < 60$ MeV.

No data events are selected with the selection criteria described above. The detection efficiency for $e^+e^- \rightarrow \eta' \rightarrow \pi^+\pi^-\eta, \eta \rightarrow 2\gamma$ events is determined using Monte Carlo (MC) simulation to be $(12.2 \pm 1.2)\%$. The quoted error is systematic. For its estimation we use the results of the study of data-MC simulation difference in the measurement of the $e^+e^- \rightarrow \pi^+\pi^-\eta$ cross section [12] at $E_{\text{cm}} > 1.2$ GeV.

The dominant sources of background for this decay mode after applying the selection criteria are the processes $e^+e^- \rightarrow \eta\gamma, \eta \rightarrow \pi^+\pi^-\pi^0$ and $e^+e^- \rightarrow \pi^+\pi^-\pi^0\pi^0$. The number of background events is estimated using MC simulation to be 0.7 ± 0.1 and 0.10 ± 0.05 for the first and second processes, respectively. The values of the $e^+e^- \rightarrow \eta\gamma$ and $e^+e^- \rightarrow \pi^+\pi^-\pi^0\pi^0$ cross sections were taken from the measurements [13–15]. The background can be also estimated from the two-dimensional distribution shown in Fig. 3 using the assumption that the χ_η^2 and $E_{2+3,\text{char}}$ distribution are independent. The number of background events in the signal rectangle ($\chi_\eta^2 < 30, E_{2+3,\text{char}} < 60$ MeV) is estimated as $n_2n_3/n_4 \approx 1 \pm 1$, where n_2, n_3 and n_4 are the numbers of data events in the regions ($30 < \chi_\eta^2 < 60, E_{2+3,\text{char}} < 60$ MeV), ($\chi_\eta^2 < 30, E_{2+3,\text{char}} > 60$ MeV) and ($30 < \chi_\eta^2 < 60, E_{2+3,\text{char}} > 60$ MeV), respectively.

There is also the nonresonant reaction $e^+e^- \rightarrow \pi^+\pi^-\eta$ having the same final state as the process under study. This reaction proceeds through the $\rho\eta$ intermediate state and, therefore, is suppressed due to the small phase space of the final particles. Interpolating the result of the fit to the $e^+e^- \rightarrow \pi^+\pi^-\eta$ cross section measured at higher energies [12], we estimate that the nonresonant cross section at $E_{\text{cm}} = 960$ MeV is about 1.7 pb. Assuming the same detection efficiencies for the resonant and nonresonant processes, the nonresonant contribution is estimated to be 0.2 events.

B. Decay chain $\eta' \rightarrow \pi^+\pi^-\eta, \eta \rightarrow 3\pi^0$

In this decay mode the following selection criteria are used. An event must contain two charged particles originating from the interaction region and six photons. We require the muon-system veto, $|180 - |\phi_1 - \phi_2|| > 10^\circ$, $\psi_{c\gamma} > 20^\circ$, $0.5 < E_{\text{cal}}/E_{\text{cm}} < 0.9$, and $E_{2+3,\text{char}} < 90$ MeV.

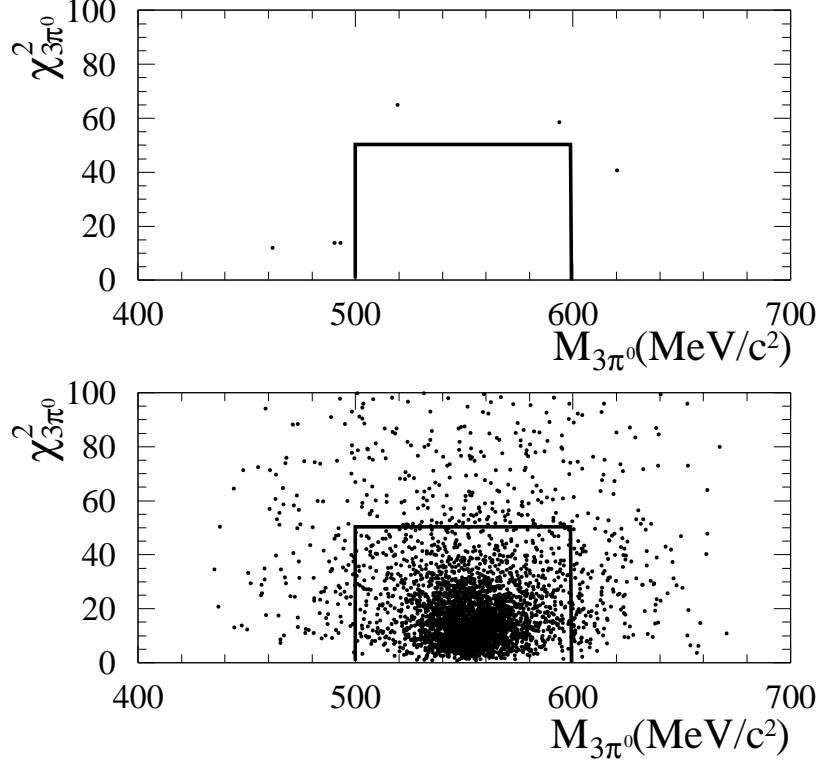


FIG. 4: The two-dimensional distribution of the parameters $\chi^2_{3\pi^0}$ and $M_{3\pi^0}$ for data events (top) and simulated $\eta' \rightarrow \pi^+\pi^-\eta, \eta \rightarrow 3\pi^0$ events (bottom). The rectangle corresponds to the selection criteria used: $\chi^2_{3\pi^0} < 50$ and $500 < M_{3\pi^0} < 600 \text{ MeV}/c^2$.

For selected events the kinematic fit is performed to the hypothesis $e^+e^- \rightarrow \pi^+\pi^-3\pi^0$. The two-dimensional distributions of χ^2 of the kinematic fit ($\chi^2_{3\pi^0}$) versus the three π^0 invariant mass ($M_{3\pi^0}$) for data events and simulated events of $e^+e^- \rightarrow \eta' \rightarrow \pi^+\pi^-\eta, \eta \rightarrow 3\pi^0$ process are shown in Fig. 4. The following cuts on these parameters are used: $\chi^2_{3\pi^0} < 50$ and $500 < M_{3\pi^0} < 600 \text{ MeV}/c^2$. No data events satisfying the selection criteria applied are found. The detection efficiency for $e^+e^- \rightarrow \eta' \rightarrow \pi^+\pi^-\eta, \eta \rightarrow 3\pi^0$ events determined using MC simulation is $(7.5 \pm 0.8)\%$. The quoted error is estimated according to Ref. [12].

It is necessary to note that the same final state $\pi^+\pi^-3\pi^0$ can be obtained in the other decay chain $\eta' \rightarrow \pi^0\pi^0\eta, \eta \rightarrow \pi^+\pi^-\pi^0$. The distribution of the three- π^0 invariant mass for this decay channel is shown in Fig. 5.

It is seen that a significant part of $\eta' \rightarrow \pi^0\pi^0\eta, \eta \rightarrow \pi^+\pi^-\pi^0$ events satisfies the condition $500 < M_{3\pi^0} < 600 \text{ MeV}/c^2$. The detection efficiency for this channel calculated using MC simulation is $(4.9 \pm 0.5)\%$. We could not increase the detection efficiency for $\eta' \rightarrow \pi^0\pi^0\eta, \eta \rightarrow$

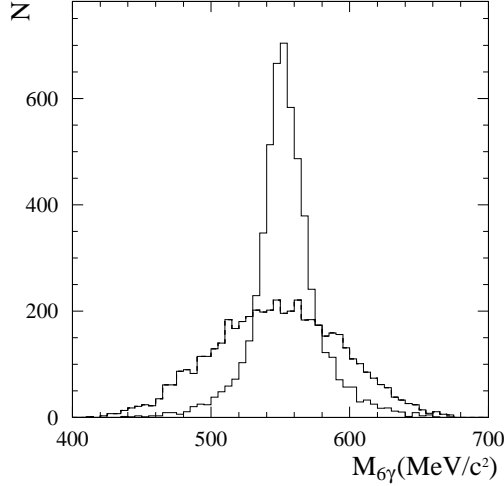


FIG. 5: The distribution of the three- π^0 invariant mass for the decay channels: $\eta' \rightarrow \pi^+\pi^-\eta$, $\eta \rightarrow 3\pi^0$ (narrow distribution) and $\eta' \rightarrow \pi^0\pi^0\eta$, $\eta \rightarrow \pi^+\pi^-\pi^0$ (wide distribution), obtained using MC simulation.

$\pi^+\pi^-\pi^0$ events by using conditions on parameters specific for this decay mode, for example, the $\pi^+\pi^-\pi^0$ invariant mass instead of $M_{3\pi^0}$.

The dominant background source for the $\pi^+\pi^-\pi^0\pi^0\pi^0$ final state is the process $e^+e^- \rightarrow \pi^+\pi^-\pi^0\pi^0$. Additional fake photons can appear as a result of nuclear interaction of charged pions or beam background. The number of background events obtained using MC simulation is 2.7 ± 0.5 . Since appearance of two fake photons is needed, the simulation can be used only for rough estimation of the background level. The background can be also estimated using the $M_{3\pi^0}$ distribution for data. Based on four observed data events with $\chi^2_{3\pi^0} < 50$ in Fig. 4 and assuming a linear background $M_{3\pi^0}$ distribution, we estimate the background in the interval $500 < M_{3\pi^0} < 600$ MeV/ c^2 to be 2 ± 1 events. The nonresonant background from the $e^+e^- \rightarrow \pi^+\pi^-\eta$ process discussed above in Sec. III A is about 0.1 events in this decay mode.

C. Decay chain $\eta' \rightarrow \pi^0\pi^0\eta$, $\eta \rightarrow \gamma\gamma$

The event selection in this decay mode is performed in two steps. At the first stage six-photon events containing no tracks in the drift chamber are selected. Each photon is required to have the transverse energy distribution in the calorimeter consistent with the distribution for an electromagnetic shower [16]. The total energy deposition E_{cal} and the

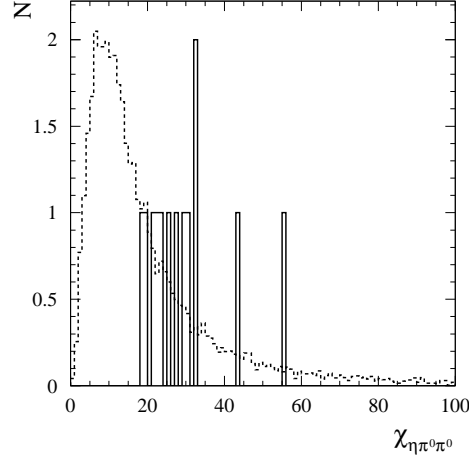


FIG. 6: The $\chi_{\eta\pi^0\pi^0}^2$ distribution for data events (solid histogram) and simulated $e^+e^- \rightarrow \eta' \rightarrow 2\pi^0\eta \rightarrow 6\gamma$ events (dashed histogram).

event momentum P_{cal} calculated using energy depositions in the calorimeter crystals must satisfy the following conditions:

$$0.7 < E_{\text{cal}}/E_{\text{cm}} < 1.2, \quad cP_{\text{cal}}/E_{\text{cm}} < 0.3, \quad E_{\text{cal}}/E_{\text{cm}} - cP_{\text{cal}}/E_{\text{cm}} > 0.7. \quad (3)$$

To reject cosmic-ray background the muon-system veto is required.

For events passing initial selection the kinematic fit to the $e^+e^- \rightarrow \eta' \rightarrow \eta\pi^0\pi^0 \rightarrow 6\gamma$ hypothesis is performed. The quality of the fit is characterized by the parameter $\chi_{\eta\pi^0\pi^0}^2$. The distributions of this parameter for data events and simulated events of the $e^+e^- \rightarrow \eta' \rightarrow \pi^0\pi^0\eta \rightarrow 6\gamma$ process are shown in Fig. 6. The condition $\chi_{\eta\pi^0\pi^0}^2 < 15$ is applied.

No data events satisfying the criteria described above have been found. The detection efficiency for the $e^+e^- \rightarrow \eta' \rightarrow \pi^0\pi^0\eta$, $\eta \rightarrow \gamma\gamma$ process obtained using MC simulation is $(14.6 \pm 0.7)\%$. The quoted error is systematic, estimated using our work [17] on the measurement of the $e^+e^- \rightarrow \pi^0\pi^0\gamma$ cross section.

The main background sources for this decay mode are the processes $e^+e^- \rightarrow \eta\gamma \rightarrow 3\pi^0\gamma$ and $e^+e^- \rightarrow \pi^0\pi^0\gamma$. Their cross sections were measured in Refs. [13, 14, 21, 22] and in this paper (see Sec. IV). The number of background events from these sources is calculated to be 1.3 ± 0.3 and 0.4 ± 0.1 , respectively. It should be noted that the number of data events with $\chi_{\eta\pi^0\pi^0}^2 < 100$ equal to 13 is in good agreement with the background prediction based on MC simulation: 12 ± 2 for $e^+e^- \rightarrow \eta\gamma$ and 3 ± 1 for $\pi^0\pi^0\gamma$.

D. Decay chain $\eta' \rightarrow \pi^0 \pi^0 \eta$, $\eta \rightarrow 3\pi^0$

For this decay mode with ten photons in the final state there is no background from e^+e^- annihilation. The main source of background is cosmic-ray showers. We select events containing nine or more photons and no tracks in the drift chamber. The photons must have the transverse energy distribution in the calorimeter consistent with the distribution for an electromagnetic shower. The parameters E_{cal} and P_{cal} must satisfy the conditions (3). The muon system signal is required to suppress cosmic-ray background. No data events are selected after applying these criteria. The detection efficiency for this decay mode is $(22.6 \pm 1.1)\%$.

IV. UPPER LIMIT FOR $\eta' \rightarrow e^+e^-$ DECAY

The visible cross section for the process $e^+e^- \rightarrow \eta'$ is calculated as follows

$$\sigma_{\text{vis}}^{\text{exp}} = \frac{N_s}{\sum L_i \varepsilon_i}, \quad (4)$$

where N_s is the sum of experimental events selected in the five decay modes, ε_i is the detection efficiency in the mode i , which includes the branching fractions for the corresponding η' and η decays. The integrated luminosity L_i is equal to $L_{ee} = 2.91 \text{ pb}^{-1}$ for the decay modes with charged particles and $L_{\gamma\gamma} = 2.82 \text{ pb}^{-1}$ for the multiphoton modes. The denominator in the formula (4) can be represented as $L_{ee}\varepsilon_s$. For the selection criteria described in the previous section $\varepsilon_s = (6.2 \pm 0.4)\%$. Since the number of selected data events is equal to zero, we set the upper limit on the cross section. The technique of Cousins and Highland [18] following the implementation of Barlow [19] is used to calculate the limit with all uncertainties included ($N_s < 2.32$ for 90% CL):

$$\sigma_{\text{vis}}^{\text{exp}} < 12.7 \text{ pb at 90\% CL.} \quad (5)$$

The limit on the cross section is translated using Eq.(2) to the upper limit on the η' electronic width

$$\Gamma_{\eta' \rightarrow e^+e^-} < 0.0020 \text{ eV at 90\% CL.} \quad (6)$$

As a test, we perform measurements of the cross sections for the processes $e^+e^- \rightarrow \pi^+\pi^-\pi^0$, $e^+e^- \rightarrow \pi^0\pi^0\gamma$ and $e^+e^- \rightarrow \eta\gamma \rightarrow 3\pi^0\gamma$. The process $e^+e^- \rightarrow \eta\gamma$ was studied in

the seven-photon final state. The events of these processes are selected with criteria similar to those described in the previous section. The obtained Born cross sections $\sigma(e^+e^- \rightarrow \pi^+\pi^-\pi^0) = 11.7 \pm 0.2$ nb, $\sigma(e^+e^- \rightarrow \pi^0\pi^0\gamma) = 285 \pm 21$ pb, $\sigma(e^+e^- \rightarrow \eta\gamma) = 244 \pm 30$ pb are in good agreement with the results of the previous measurements 11.33 ± 0.64 nb [20] for $e^+e^- \rightarrow \pi^+\pi^-\pi^0$, 242_{-67}^{+89} pb [21] and 390_{-98}^{+112} pb [22] for $e^+e^- \rightarrow \pi^0\pi^0\gamma$, 300 ± 110 pb [13] and 390_{-110}^{+140} pb [14] for $e^+e^- \rightarrow \eta\gamma$.

V. CONCLUSION

The search for the process $e^+e^- \rightarrow \eta'$ has been performed in the experiment with the SND detector at the VEPP-2000 e^+e^- -collider. To reconstruct the η' -meson the five decay chains have been used: $\eta' \rightarrow \eta\pi^+\pi^-$ followed by the η decays to $\gamma\gamma$ and $3\pi^0$, and $\eta' \rightarrow \eta\pi^0\pi^0$ with η decays into $\pi^+\pi^-\pi^0$, $\gamma\gamma$, and $3\pi^0$. No data events of the $e^+e^- \rightarrow \eta'$ process have been found. Since the visible cross section for the process under study is proportional to the η' electronic width, we set the upper limit

$$\Gamma_{\eta' \rightarrow e^+e^-} < 0.0020 \text{ eV at 90\% CL.} \quad (7)$$

The obtained limit is slightly better than the limit set recently in the CMD-3 experiment $\Gamma_{\eta' \rightarrow e^+e^-} < 0.0024$ eV [6].

Using the formula (4) we combine the SND (0 events, $L_i = 2.91$ pb $^{-1}$, $\varepsilon_i = (6.2 \pm 0.4)\%$) and CMD-3 (0 events, $L_i = 2.69$ pb $^{-1}$, $\varepsilon_i = (5.3 \pm 0.3)\%$) data and obtain the combined upper limits on the electronic width

$$\Gamma_{\eta' \rightarrow e^+e^-} < 0.0011 \text{ eV at 90\% CL.} \quad (8)$$

and the branching fraction $[\Gamma_{\eta'} = (0.198 \pm 0.009) \text{ MeV [10]]}$

$$\mathcal{B}(\eta' \rightarrow e^+e^-) < 5.6 \times 10^{-9} \text{ at 90\% CL.} \quad (9)$$

The obtained upper limit is most stringent but still 30-50 times larger than theoretical predictions [2, 3] made in the framework of the Standard Model.

VI. ACKNOWLEDGMENTS

We thank S.I. Eidelman for fruitful discussions. Part of this work related to the photon reconstruction algorithm in the electromagnetic calorimeter and analysis of multiphoton

events is supported by Russian Science Foundation (project N 14-50-00080). This work is partly supported by the RFBR grant No. 15-02-03391.

-
- [1] S. M. Berman and D. A. Geffen, *Nuovo Cimento* **18**, 1192 (1960).
 - [2] T. Petri, arXiv:1010.2378 [nucl-th].
 - [3] A.E. Dorokhov, *Phys. Part. Nucl. Lett.* **7**, 229 (2010).
 - [4] Y. Kahn, M. Schmitt and T. M. P. Tait, *Phys. Rev. D* **78**, 115002 (2008).
 - [5] Q. Chang and Y. D. Yang, *Phys. Lett. B* **676**, 88 (2009).
 - [6] R. R. Akhmetshin *et al.* (CMD-3 Collaboration), *Phys. Lett. B* **740**, 273 (2015).
 - [7] P. V. Vorobev *et al.* (ND Collaboration), *Sov. J. Nucl. Phys.* **48**, 273 (1988) [*Yad. Fiz.* **48**, 436 (1988)].
 - [8] Yu. M. Shatunov *et al.*, in Proceedings of the 7th European Particle Accelerator Conference, Vienna, 2000, p. 439, <http://accelconf.web.cern.ch/AccelConf/e00/PAPERS/MOP4A08.pdf>.
 - [9] M. N. Achasov *et al.*, *Nucl. Instrum. Methods Phys. Res., Sect. A* **598**, 31 (2009); V. M. Aulchenko *et al.*, *ibid.* **598**, 102 (2009); A. Yu. Barnyakov *et al.*, *ibid.* **598**, 163 (2009); V. M. Aulchenko *et al.*, *ibid.* **598**, 340 (2009).
 - [10] K. A. Olive *et al.* (Particle Data Group), *Chin. Phys. C* **38**, 090001 (2014).
 - [11] E. V. Abakumova *et al.*, *Nucl. Instrum. Meth. A* **744**, 35 (2014).
 - [12] V. M. Aulchenko *et al.* (SND Collaboration), *Phys. Rev. D* **91**, 052013 (2015).
 - [13] R. R. Akhmetshin *et al.* (CMD-2 Collaboration), *Phys. Lett. B* **509**, 217 (2001).
 - [14] M. N. Achasov *et al.* (SND Collaboration), *Phys. Rev. D* **76**, 077101 (2007).
 - [15] M. N. Achasov *et al.* (SND Collaboration), *J. Exp. Theor. Phys.* **109**, 379 (2009).
 - [16] A. V. Bozhenok, V. N. Ivanchenko and Z. K. Silagadze, *Nucl. Instrum. Methods Phys. Res., Sect. A* **379**, 507 (1996).
 - [17] M. N. Achasov *et al.* (SND Collaboration), *Phys. Rev. D* **88**, 054013 (2013).
 - [18] R. D. Cousins and V. L. Highland, *Nucl. Instrum. Methods Phys. Res., Sect. A* **320**, 331 (1992).
 - [19] R. Barlow, *Comput. Phys. Commun.* **149**, 97 (2002).
 - [20] M. N. Achasov *et al.* (SND Collaboration), *Phys. Rev. D* **68**, 052006 (2003).
 - [21] M. N. Achasov *et al.* (SND Collaboration), *Phys. Lett. B* **537**, 201 (2002).

- [22] R. R. Akhmetshin *et al.* (CMD-2 Collaboration), Phys. Lett. B **580**, 119 (2004).